Dynamic Consensus Algorithm Based Distributed Global Efficiency Optimization of a Droop Controlled DC Microgrid

Meng, Lexuan; Dragicevic, Tomislav; Guerrero, Josep M.; Vasquez, Juan Carlos

Published in:
Proceedings of the 2014 IEEE International Energy Conference (ENERGYCON)

DOI (link to publication from Publisher):
10.1109/ENERGYCON.2014.6850587

Publication date:
2014

Document Version
Early version, also known as pre-print

This document is a preprint of the final paper:
L. Meng, T. Dragicevic, J. M. Guerrero, "Dynamic consensus algorithm based distributed global efficiency optimization of a droop controlled dc microgrid," in Proc. IEEE International Energy Conference (EnergyCon'14), 2014.

Dynamic Consensus Algorithm Based Distributed Global Efficiency Optimization of a Droop Controlled DC Microgrid

Lexuan Meng, Tomislav Dragicevic, Josep M. Guerrero, Juan C. Vasquez

Denmark Microgrids Research Programme www.microgrids.et.aau.dk

Department of Energy Technology, Aalborg University
Pontoppidanstræde 101, Aalborg, Denmark
{lme,tdr,joz,juq}@et.aau.dk

***Abstract*—In a DC microgrid, several paralleled conversion systems are installed in distributed substations for transferring power from external grid to a DC microgrid. Droop control is used for the distributed load sharing among all the DC/DC converters. Considering the typical efficiency feature of power electronic converters, optimization method can be implemented in tertiary level for improving the overall system efficiency. However, optimization purposes usually require centralized communication, data acquisition and computation which might be either impractical or costly for dispersed systems. Accordingly, this paper proposes a dynamic consensus algorithm based distributed optimization method aiming at improving the system efficiency while offering higher expandability and flexibility when compared to centralized control. Hardware-in-the-loop (HIL) results are shown to demonstrate the effectiveness of the method.**

***Keywords:* DC microgrid, dynamic consensus algorithm, distributed optimization, droop control, dc/dc converter.**

I. INTRODUCTION

In a direct current (DC) microgrid, as shown in Fig. 1, four distributed substations are established for extracting power from energy resources to supply the load in the microgrid. In this paper, the energy resources are assumed to be alternate current (AC) grids. Four two-stage conversion systems are working in parallel. The AC/DC converter stage uses uncontrolled rectifier for transferring AC power to DC power from external AC grids. A DC/DC converter stage is implemented in cascade with the front AC/DC stage. The DC/DC converters can be regulated so as to control the power flow between the external grid and the microgrid. The power sharing among converters becomes critical issue in this case where droop control method can be applied so as to achieve communication-less automatic power sharing [1]–[5].

Conventionally, the converters are assigned static droop coefficients, which realize the fixed proportion of load current sharing [1], [2]. However, taking into account that the efficiency of the converters is typically changing with their output currents [6], the global efficiency optimum is not guaranteed by applying static droop method [4]. Instead, a more convenient solution can be to adjust the current sharing proportion among converters under different load conditions so as to ensure the maximized overall efficiency. In line with this, centralized optimization was implemented in [4] for system overall efficiency enhancement.

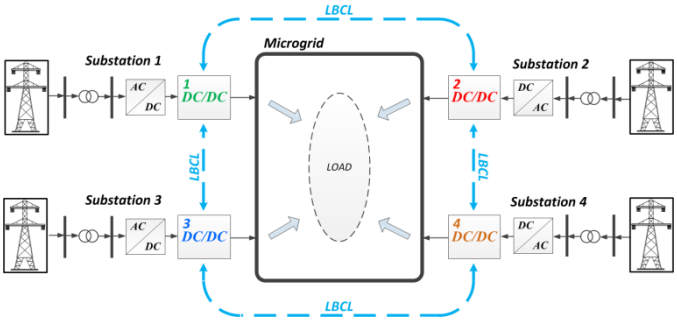

Fig. 1. Case study: DC microgrid system

However, for distributed systems it is either impractical or costly to have a central control system with communication links connected to each local unit [7]–[9]. Besides, there are several well-known pitfalls associated with centralized optimization, i.e. single point of failure, limited flexibility and difficult expandability [9]. In order to avoid these drawbacks, a distributed decision-making and optimization scheme is needed. Distributed algorithms [10], such as consensus algorithms [11], can be possible solutions for global information discovery in a distributed fashion.

The general purpose of consensus algorithms is to allow a set of agents to reach an agreement on a quantity of interest by exchanging information through communication network [11]. These kinds of agents are only required to communicate with their neighbors. A distributed decision-making based on a dynamic consensus algorithm was implemented in this paper [12] for automatic load restoration. The global information is discovered by each agent knowing the current state of the generation and consumption in all the buses. Local decision for loads restoration can be made according to the priority of the loads. In addition, the plug-and-play function for seamless connection of new units was designed. Similar approach is applied also in [13] for balancing the generation and consumption by coordinating the operation of doubly-fed induction generators. Considering the localized generation, storage and consumption feature of future smart grid, wireless communication network is generally accepted as highly flexible and low cost way for facilitating the control and monitoring in microgrids. Accordingly, a consensus theory

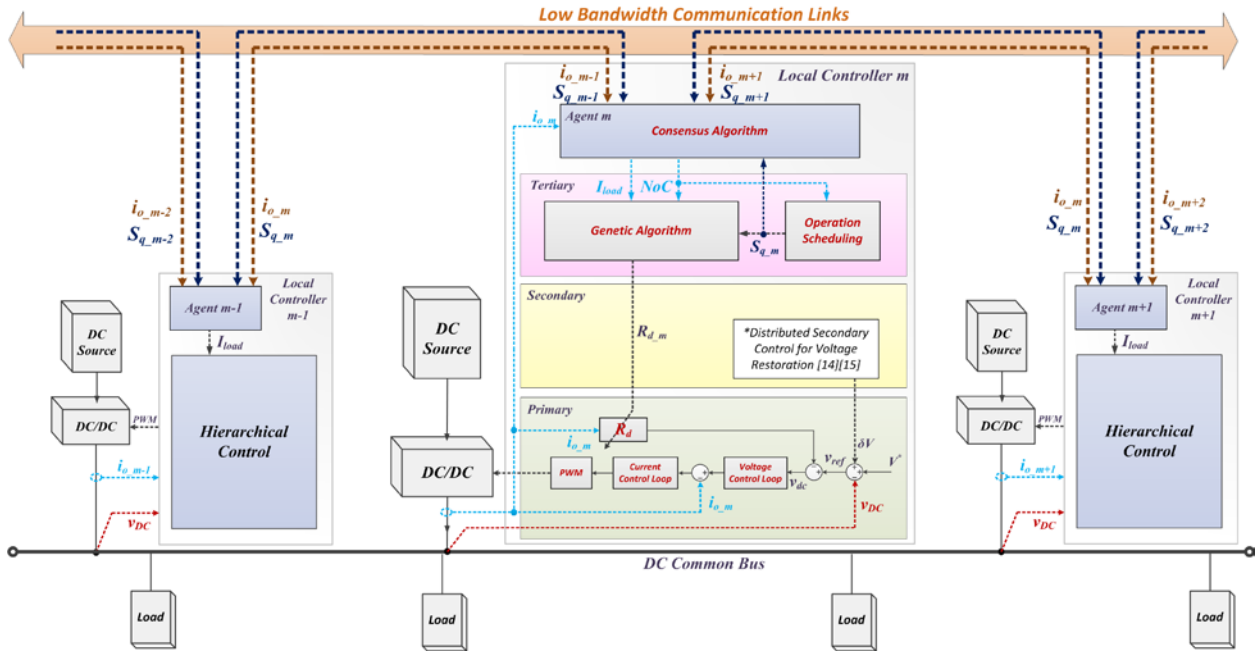

Fig. 2. Distributed hierarchical control and communication structure

based distributed coordination scheme for microgrid via wireless communication is proposed in [14] for coordinating the generation, storage and consumption.

In order to perform distributed optimization, this paper applies a dynamic consensus algorithm for global information sharing. The paper is organized as follows. The distributed hierarchical control structure is described in Section II with information consensus layer, tertiary control layer, secondary control layer and primary control layer differentiated. Section III introduces the dynamic consensus algorithm applied in this paper for obtaining the information about the total load current. Stability of the algorithm is also analyzed. Based on the analysis of system overall efficiency the optimization problem is formulated in Section IV. In order to adjust the current sharing ratio, an adaptive virtual resistance method is introduced in Section V with small signal stability analysis. HiL results are shown in Section VI to verify the effectiveness of the method.

II. Distributed Hierarchical Control

Hierarchical control was proposed for proper control of microgrid systems [1], [2]. The three layers, namely tertiary, secondary and primary, are designed to achieve control objectives in different time scales and with different significances. As power electronic equipment is widely used for interfacing energy resources into microgrid system, power sharing methods, such as droop control, are usually applied in primary level for controlling the power injection of each energy resource. Secondary control deals with power quality issues, such as voltage and frequency restoration, unbalance and harmonics compensation. Tertiary control takes care of system level regulation issues, such as optimal power flow, economic operation, scheduling and so forth. Tertiary control has much slower control speed compared with secondary and primary control.

Primary control is commonly installed at each local controller, while the way of implementing secondary and tertiary can be centralized or distributed [1], [5], [7], [15], [16]. They both have advantages and disadvantages. Centralized secondary and tertiary controls are usually installed in microgrid central controller (MGCC). It provides a strong supervision over the whole system and facilitates the function of global regulation and optimization. However, this option needs extensive communication infrastructure which causes higher cost and lower reliability. Also the flexibility and expandability of centralized control is limited since the supervisory controller needs to be reprogrammed for every new unit. It is more suitable for centralized or small scale systems [8], [9]. On the other hand, decentralized control tends to perform secondary and tertiary control in each local controller. Communication links are then only required between neighboring units. Information sharing and consensus algorithm is needed for each local controller to obtain environment information so as to perform decision-making functions, also named multi-agent systems [8], [9], [17], [18]. Compared with centralized control, this option saves the cost of implementing large length of communication links, avoids the halt of the whole system caused by a single point failure in MGCC or communication links, and improves the system flexibility and expandability. However, the system security is sacrificed because of the lack of strong centralized supervision. Also it is more difficult to perform decentralized optimization for each local controller to achieve a global objective. It is more suitable for largely dispersed system and each of the local units has its own goals, e.g. cost and profit.

In order to implement optimization method in a system with largely dispersed units for achieving the enhancement of

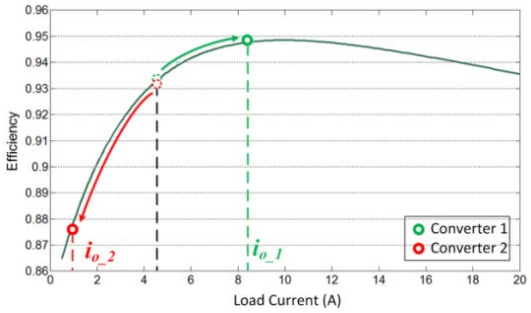

Fig. 3. Typical converter efficiency curve

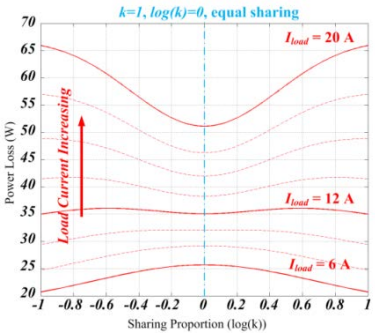

Fig. 4. System power loss P_{TL} changing with sharing proportion

overall system efficiency, this paper proposes distributed hierarchical control architecture as shown in Fig. 2. A number of converters and its local control systems (index number 1, 2, …, *m*, …, N_{oC}, N_{oC} is the total number of units) exist in the system and they communicate only with neighboring units.

The inner voltage and current control loops as well as the droop control loop are integrated in primary level. Droop control loop appears as a virtual impedance (VR, R_d) over voltage control loop [2]:

$$v_{dc} = v_{ref} - R_{d\_m} \cdot i_{o\_m} \tag{1}$$

where i_{o_m} and R_{d_m} are the output current and VR value of the m^{th} unit, and v_{ref} is the output voltage reference at no load. Usually VR is fixed by the maximum allowed voltage deviation ε_v and maximum output current i_{max}:

$$R_d = \varepsilon_v / i_{\max} \tag{2}$$

This paper applies a dynamic VR shifting method for changing the output current of each converter to a desirable value [4].

Secondary control loops deals with the restoration of voltage deviation caused by droop control. Distributed secondary control [15], [16] is required for this system which is out of the scope of this paper.

Optimization method is implemented in tertiary level for optimizing the operation of each converter so as to achieve enhancement of overall system efficiency [4]. An operation scheduling block is also included in tertiary level for distributing the workload among all the converters.

However, as the overall system efficiency is a global objective, the total load current is required for performing the optimization function. A dynamic consensus algorithm (DCA) [11], [19] is applied in this paper for obtaining the total load current. The optimization method and consensus algorithm are introduced in the following sections.

III. System Efficiency Analysis and Optimization

For paralleled DC/DC converter system, the losses are mainly related with conversion losses which are caused by switching, driver and filter parasitic elements in each converter [6]. Even if constant input and output voltages are assumed, efficiency of each converter changes with its output current, as shown in Fig. 3. Two paralleled 1kW DC/DC converters are taken as example here, their maximum output current is 20A with nominal input/output voltage of 100/48V. As the efficiency is usually relatively much lower in light load conditions, there exists a room for optimization, which is to find the power sharing proportion under different load conditions where the losses of the system are minimized.

A. System Efficiency Analysis and Optimization Problem Formulation

A typical theoretical efficiency curve is shown in Fig. 3. *Matlab Curve Fitting Tool* is used to transform data into function:

$$\eta(i) = 0.975 \cdot e^{-2\times10^{-3}\cdot i} - 0.1257 \cdot e^{-0.3\cdot i} \tag{3}$$

where η is converter efficiency and i is converter output current. Then, the power conversion losses of a system with n paralleled converters may be calculated as follows:

$$P_{TL} = \sum_{m=1}^{N} V_{DC} \cdot i_{o\_m} \cdot \frac{1-\eta_m}{\eta_m} \tag{4}$$

where V_{DC} is dc bus voltage, i_{o_m} is the output current of j^{th} converter, and η_m is the efficiency of m^{th} converter. Minimization of total conversion losses, P_{TL}, is taken as the objective in the following optimization problem.

Assuming two converters share the load current as the green and red points shown in Fig. 3. In light load conditions, it is more efficient to differentiate the sharing proportion so as to enhance the system efficiency. A sharing gain is defined as:

$$\begin{cases} k = \dfrac{i_{o\_1}}{i_{o\_2}} \\ i_{o\_1} + i_{o\_2} = I_{load} \end{cases} \tag{5}$$

Fig. 4 shows the changing of system power losses with regard to logarithm of sharing proportion k under different load conditions. It can be seen that, under light load conditions (I_{load}<12A), the system losses are much lower when the sharing proportion k is larger. It means that it is more efficient to differentiate the load current sharing proportion of operating converters under light load conditions.

B. Adaptive Virtual Resistance Method

In order to change the output current of each converter, the VR, R_d, can be adjusted as shown in Fig. 5. From (1), the output current of each converter can be calculated as:

$$i_{o\_m} = \frac{v_{ref} - v_{dc}}{R_{d\_m}} \tag{6}$$

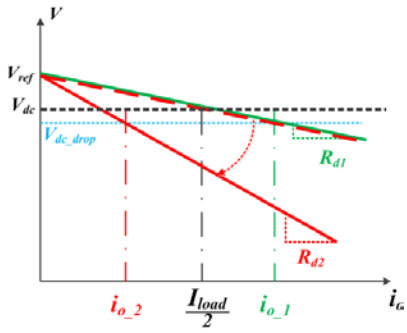

Fig. 5. System power loss P_{TL} changing with sharing proportion

As v_{ref} and v_{dc} are the same for all the converters, the ratio of the output current of converters is proportional to the reciprocal of VRs:

$$i_{o\_1} : i_{o\_2} : \ldots : i_{o\_N_{oC}} = \frac{1}{R_{d\_1}} : \frac{1}{R_{d\_2}} : \ldots : \frac{1}{R_{d\_N_{oC}}} \tag{7}$$

Accordingly, the optimization objective is to find an optimal sharing proportion among all the converters so as to minimize the system losses (P_{TL}). VRs can be used as decision variables for adjusting the relative sharing proportion of load current among all the converters.

However, the change of VRs certainly has influence on common DC bus voltage and control system dynamics. The voltage deviation caused by droop control and VR shifting can be fast restored by secondary control, and this part is out of the scope of this paper.

The small signal stability analysis is necessarily needed for properly set the shifting range of VRs so as to ensure the system stability. The dynamic model of a paralleled buck converter system (4 converters) is shown in Fig. 6. Voltage and current loops can be accomplished by conventional *PI* controllers. VR appears as a proportional current feedback over inner control loops. Each converter along with its primary control system can be described as following model:

$$\begin{cases} v_{DC}^{*} = V^{*} + \delta V - v_{DC} - R_d \cdot i_L \\ i_{ref} = (\dfrac{K_{Iv}}{s} + K_{Pv}) \cdot v_{DC}^{*} \\ D = (\dfrac{K_{Ic}}{s} + K_{Pc}) \cdot (i_{ref} - i_L) \\ L\dfrac{di_L}{dt} = v_{in} \cdot D - v_{DC} - R_p \cdot i_L \\ C\dfrac{dv_{DC}}{dt} = \sum i_L - \dfrac{1}{R_{load}} \cdot v_{DC} \end{cases} \tag{8}$$

where V^{*} is the fixed voltage reference, δV is the voltage deviation compensating reference given by secondary controller, i_L and v_{DC} are the converter inductor current and capacitor voltage respectively. K_{Pv}, K_{Pc}, K_{Iv} and K_{Ic} are the control parameters of voltage and current loop *PI* controllers. L and C are inductance and capacitance of the converter output filter, R_p is the parasitic resistance of the filter, R_{load} is

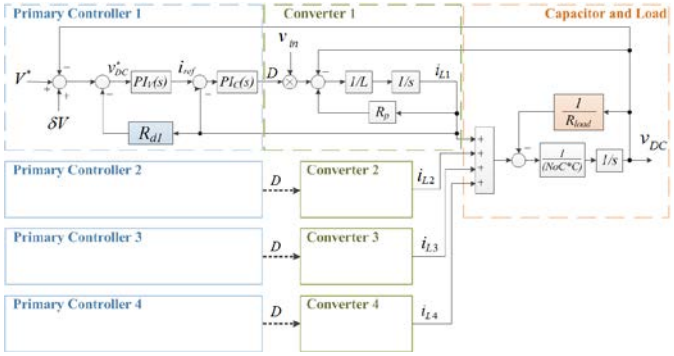

Fig. 6. Dynamic model of paralleling converter system

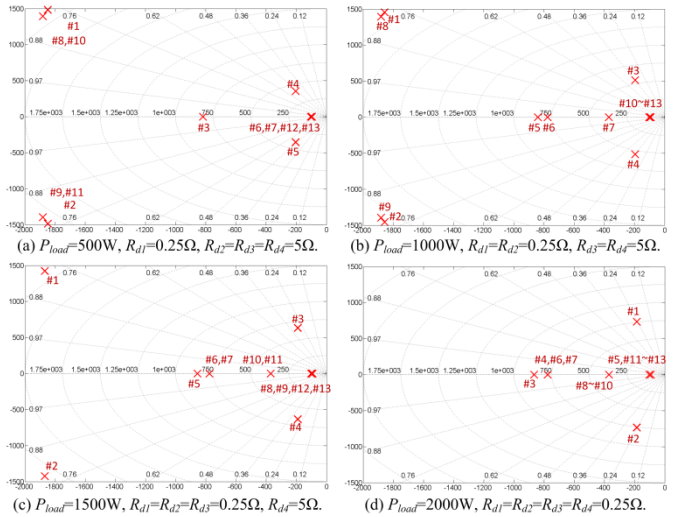

Fig. 7. Dynamic model of paralleling converter system

the equivalent resistance of the total load, v_{in} is the source voltage, D is the duty ratio.

Eq. (8) can be rewritten in a more compact state space model defined as:

$$\dot{x}_s = A_s \cdot x_s + B_s \cdot u \tag{9}$$

where all the modules share the common part of capacitor and load. In the state space model, there are two state variables in each primary controller, one state variable in each converter stage, and one common state variable in the capacitor and load part. As a result, in the system with *NoC* converters, the total number of state variables is (3*N_{oC}+1), This number is also the number of eigenvalues of the state matrix A_s.

Assume a study case in which four 1kW buck converters are working in parallel supplying a microgrid, the eigenvalues of the state matrix are plotted as shown in Fig. 7. The total number of eigenvalues is 13. The shifting range of VR is set to 0.25 to 5, and four different load conditions are considered in this analysis: P_{load}=500W, 1000W, 1500W, 2000W. At light load condition (P_{load}=500W), the VRs of the four converters are set to R_{d1}=0.25Ω, R_{d2}=R_{d3}=R_{d4}=5Ω, which means at light load conditions one of the four converters supplies most part of the total load current. It can be seen from Fig. 7 (a) that all the eigenvalues are located at the left half plane, the system is assumed to be stable. Similar conclusion can be obtained under the other load conditions according to

Fig. 7 (b)~(d). Accordingly, it is feasible to adjust the VRs between 0.25~5 while the system stability is also ensured.

C. Optimization Problem Formulation

Based on the analysis above, the optimization problem can be formulated as:

$$obj.: Min\{P_{TL}\} \tag{10}$$

$$dec.var.: \{R_{d\_1}, R_{d\_2}, ..., R_{d\_m}, ..., R_{d\_N_{oC}}\} \tag{11}$$

$$s.t.: \begin{cases} 0.25 \le \{R_{d\_1}, R_{d\_2}, ..., R_{d\_m}, ..., R_{d\_N_{oC}}\} \le 5 \\ \{i_{o\_1}, i_{o\_2}, ..., i_{o\_m}, ..., i_{o\_N_{oC}}\} \le I_{MAX} \end{cases} \tag{12}$$

where the objective is the minimization of P_{TL}, the decision variables are VRs *of the* , I_{MAX} is the maximum conversion current limit of each converter. The ratio of output current among converters is equal to the ratio of reciprocal of their VRs. The implementation and parameter tuning which guarantee the convergence of the optimization algorithm were introduced in [4].

D. Operation Scheduling

As it is shown in above analysis, the optimization is actually to find an optimal sharing proportion among all the converters. However, the converter which is always turned on may experience more rapid wear&tear than the other ones. Accordingly, a scheduling procedure is added in this paper so as to distribute the workload in a given time range. Each converter is assigned a priority number (S_{q_m}=1,2,…,N_{oC}) at the beginning when it is connected to the system. The optimization results are given as an array R_D=[R_{d_1}, R_{d_2}, …, R_{d_Noc}]. A sorting procedure is also included which makes the elements of R_D in ascending sequence. The priority number of the local converter decides which element in the optimal array R_D will be sent to primary controller. In addition, S_{q_m} is shifted after each given time range so as to distribute the workload among all the converters. Also S_{q_m} can be used to inform the system the total number of online converters. This is introduced in the next section.

IV. Multi-agent Based Information Consensus

The distributed generation, conversion and consumption improve the efficiency, reliability and flexibility of future grid. However, this new paradigm also introduces obstacles for performing optimization functions, especially, to achieve global objectives such as system overall efficiency. Centralized optimization provides reliable and stable solutions, but it also brings higher cost for communication and data acquisition.

This section introduces the application of a DCA so as to achieve distributed information sharing. Low bandwidth communication links (LBCL) [20] are required only between neighboring units. The local conversion current of each unit (i_{o_m}) and the priority number (S_{q_m}) are transmitted by each agent to their neighbors. The total load current and the total number of online converters are obtained by using DCA so that each local controller can perform optimization function.

A. Dynamic Consensus Algorithm

The discrete form of information discovery algorithm can be presented as [11]:

$$x_m(k+1) = x_m(k) + \sum_{n \in N_m} a_{mn} \cdot (x_n(k) - x_m(k)) \tag{13}$$

where m=1,2,…,N_{oC}, N_{oC} is the total number of agent nodes. $x_m(k)$ and $x_m(k+1)$ are the information obtained by agent m at iteration k and $k+1$ respectively. a_{mn} is the *edge weight* between node m and node n, a_{mn}=0 if the nodes m and n are not neighboring nodes. N_m is the set of indexes of the agents that are connected with agent m.

From a system point of view, the vector form of the iteration algorithm can be expressed as [11]:

$$X(k+1) = W \cdot X(k) \tag{14}$$

with $X(k) = [x_1(k), x_2(k), ..., x_{N_{oC}}(k)]^T$ and W is the *weight matrix* of the communication network:

$$W = \begin{bmatrix} 1 - \sum_{j \in N_1} a_{1j} & \cdots & a_{1N_{oC}} \\ \vdots & \ddots & \vdots \\ a_{1N_{oC}} & \cdots & 1 - \sum_{j \in N_{NoC}} a_{N_{oC}j} \end{bmatrix} \tag{15}$$

The final consensus equilibrium X_{eq} reached is:

$$X_{eq} = \lim_{k \to \infty} X(k) = \lim_{k \to \infty} W^k X(0) = \left(\frac{1}{N_{oC}} \mathbf{1} \cdot \mathbf{1}^T \right) X(0) \tag{16}$$

where $X(0) = [z_1, z_2, ..., z_m, ..., z_{N_{oC}}]$ is the vector of the initial values hold by each agent, **1** denotes the vector with all the elements 1. The detailed proof of the convergence can be found in [11].

In addition, in order to ensure the accurate and dynamical information consensus, a modified dynamic consensus algorithm [21] is applied in this paper. With this modification, the algorithm (13) can be rewritten as:

$$x_m(k+1) = z_m + \sum_{n \in N_m} a_{mn} \cdot \delta_{mn}(k+1) \tag{17}$$

$$\delta_{mn}(k+1) = \delta_{mn}(k) + x_n(k) - x_m(k) \tag{18}$$

where $\delta_{mn}(k)$ stores the cumulative difference between two agents, and $\delta_{mn}(0) = 0$. Based on (17) and (18), it is explicit that the final consensus value depends on z_m, and regardless of any changes to z_m, the algorithm will converge to appropriate average. Also, the precise consensus can also be achieved even under dynamic change of communication topology or adding/reducing number of nodes.

B. Communication Algorithm Dynamics

The communication topology applied in this paper, and its *Laplacian* matrix (L) and *weight* matrix (W) are shown in Fig. 8. Constant edge weight (ε) is used in this case, where:

$$W = I - \varepsilon \cdot L \tag{19}$$

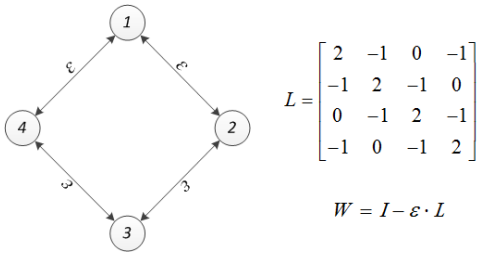

Fig. 8. Communication topology and its *Laplacian* matrix

In order to ensure the stable and fastest convergence of the communication algorithm, ε has to be properly chosen. As bidirectional communication links are considered, it is referred to as the symmetric fastest distributed linear averaging (*symmetric FDLA*) problems. The *symmetric FDLA* problem is actually the minimization of spectral radius of $W-(1/N_{oC})\cdot\mathbf{1}\cdot\mathbf{1}^T$ with certain constraints on *weight* matrix *W*. The fastest convergence is ensured when [19]:

$$\varepsilon = \frac{2}{\lambda_1(L)+\lambda_{n-1}(L)} \tag{20}$$

where $\lambda_j(\cdot)$ denotes the j^{th} largest eigenvalue of a symmetric matrix. Based on the topology of Fig. 8, the eigenvalues of L are $[0\ 2\ 2\ 4]^T$ which gives the optimal ε =1/3. The converging speed is compared in Fig. 9. Considering the limitation of communication speed, the time step of the consensus algorithm is set to 100ms which means 100ms communication time delay is considered. The system starts with $X(0)=[z_1,z_2,z_3,z_4]=[1,3,5,7]$ and converges to average value 4. At 3s, z_1 changes from 1 to 5, the new average value is 5. According to the comparison, the weight ε =1/3 is demonstrated to have minimized spectral radius $\rho(W-(1/N_{oC})\cdot\mathbf{1}\cdot\mathbf{1}^T)$ and fastest converging speed.

Furthermore, when the communication topology is forced to change, the algorithm should be able to tolerate the topology change and ensure the accurate averaging, as shown in Fig. 10. At 4s, one communication link is broken which causes oscillation of average value in each node. Around 6s, the new steady state is reached with correct average value. At 7s, z_1 changes from 5 to 3. The algorithm helps each agent discover the new average value 4.5. The above results demonstrate that the algorithm can provide accurate average value for each agent even under dynamic state change and topology change conditions.

C. Implementation of DCA

In order to perform optimization, it is necessary to know the global information of: (1) the total load current (I_{load}) and (2) the total number of online converters (N_{oC}). The total load current can be obtained by each agent node by sending the output current of the local converter to neighboring units. The equilibrium of load current calculation achieve in each agent node is the average value of the total load current:

$$i_{eq} = \frac{\sum_{m=1}^{N_{oC}} i_{o\_m}}{N_{oC}} \tag{21}$$

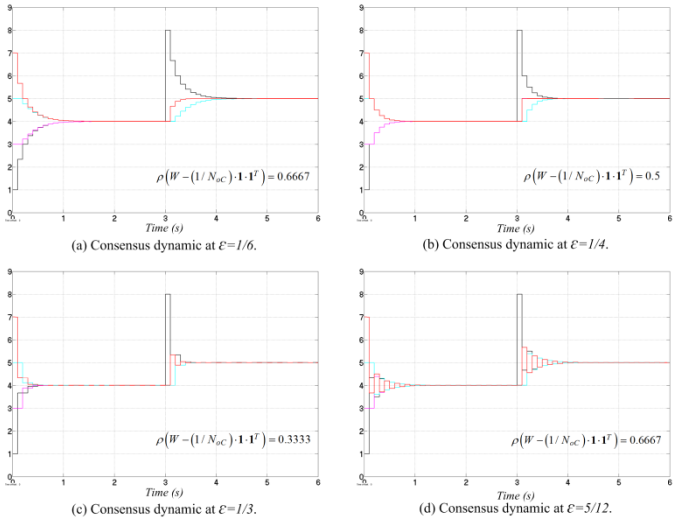

Fig. 9. Converging speed comparison under different constant weight ε.

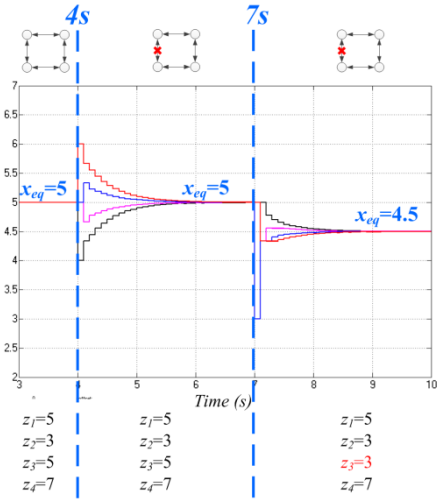

Fig. 10. Information consensus under topology change.

based on which the total load current can be calculated by multiply N_{oC} to the averaged value i_{eq}.

In order to know the number of online converters, the priority number of each converter (S_{q_m}=1,2,…,N_{oC}) is used and sent to neighboring units. The equilibrium of the priority information can be obtained as:

$$S_{eq} = \frac{\sum_{m=1}^{N_{oC}} S_{q\_m}}{N_{oC}} = \frac{\frac{N_{oC}\cdot(N_{oC}+1)}{2}}{N_{oC}} = \frac{N_{oC}+1}{2} \tag{22}$$

based on which N_{oC} can be calculated as:

$$N_{oC} = 2S_{eq} - 1 \tag{23}$$

V. Hardware-in-Loop Results

In order to verify the effectiveness of the proposed method, simulation models are established in Simulink and compiled to *dSPACE* for *HiL* simulation. The lower level controllers and averaged converter model are shown in Fig. 6. The *Genetic Algorithm* is implemented using *Matlab-Function*.

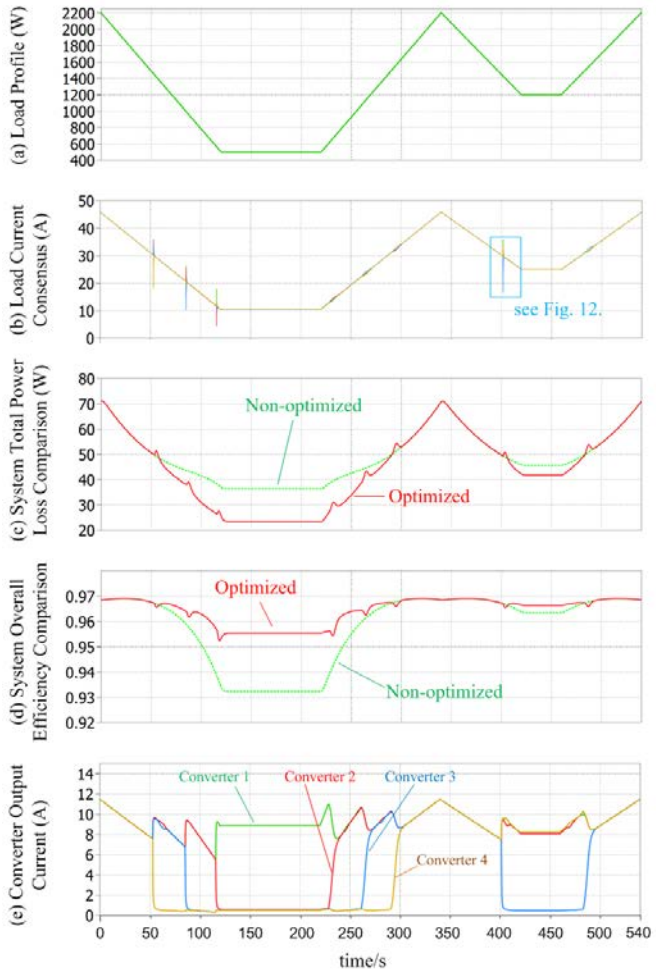

Fig. 11. One load cycle simulation results.

DCA is implemented using Simulink blocks. The control speed is differentiated in different layers considering the hardware limitations. The simulation model time-step is set to 0.1ms. The tertiary optimization is executed every 0.5s, and the DCA is executed every 100ms which means a 100ms communication delay is considered.

A. One load profile cycle

A load profile is input to the simulation model so as to obtain the response of the control system and verify the results. The load power is changing between 500W to 2200W. As the DC common bus voltage is always kept at 48V, the total load current is changing between 10A to 46A.

Fig. 11 (b) shows the total load current discovered by each agent which demonstrates that the consensus algorithm is able to help each agent obtain the accurate information. The detailed consensus dynamics are shown in Fig. 12.

The comparison between optimized and non-optimized system regarding the system overall power losses and efficiency are shown in Fig. 11 (c) and (d). It is demonstrated that the optimized system has relative lower power losses and higher system overall efficiency especially under light load conditions. Fig. 11 (e) indicates the strategy of employing

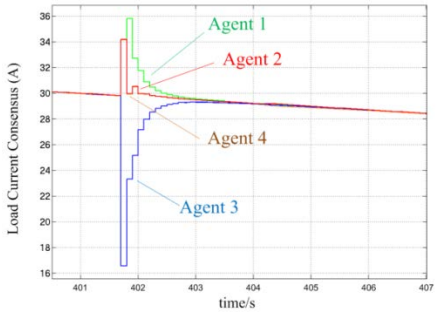

Fig. 12. Information consensus dynamics.

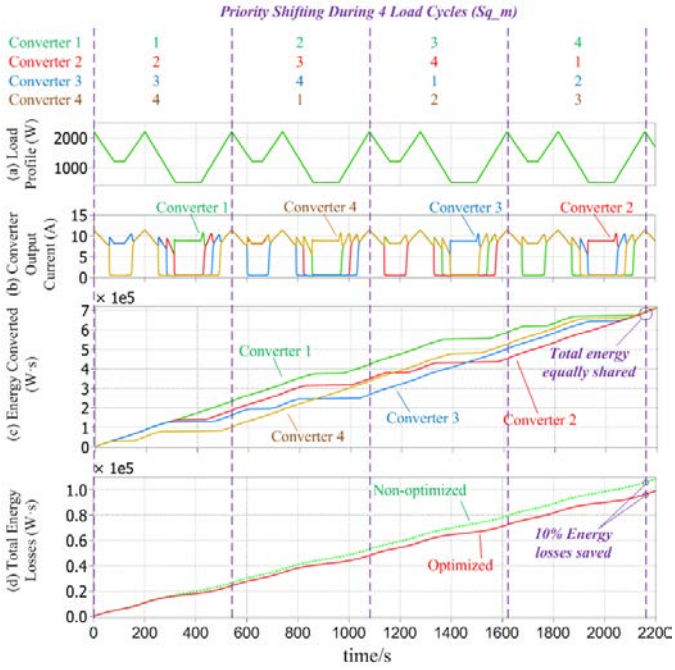

Fig. 13. 4 load cycles simulation results.

converters under different load conditions. In light load conditions, less converters are supplying.

B. Consensus dynamics

The dynamics of the consensus algorithm during changing of number of supplying converters are shown in Fig. 12. At this point, the optimization and decision making process decides to put one converter into standby mode because it is more efficiency to employ less converters. It can be seen in Fig. 11 (e) that at 401s, the current generation of converter 3 is decreased to a low level. During this process, the state of agent 3 is changed which causes an oscillation on the states of other agents as shown in Fig.12. But within 2 seconds, the algorithm is able to help all the agents re-converge to the right consensus even the load is dynamically changing at the same time. Accordingly, the system is able to adapt to this change and keeps normal operation.

C. Four load profile cycle

According to the simulation results presented in Fig. 11, one converter is undertaking most of the load current in light load conditions which may cause fast wear and tear for this converter after long term operating. An operation scheduling

and priority shifting method is necessarily needed so as to distribute the total workload. Considering that in real world system, the load profile feature is similar from day to day, the priority number (S_{q_m}) can be shifted after each cycle so as to ensure the near equalized workload distribution among all the converters. The simulation results of 4 load cycles are shown in Fig. 13. The priority number of each converter is shifted from cycle to cycle. Also this priority number can be used to obtain the information of total number of online converters as shown in (22) and (23).

Fig. 13 (b) shows the output current of each converter during different cycles. As their priority number is shifted, different converter is undertaking most of the load current in different cycle. Fig. 13 (c) demonstrates that after 4 cycle of operation, the total energy converted are equally shared among the four converters.

Fig. 13 (d) indicates that compared with non-optimized system, 10% energy losses are reduced by applying the proposed method.

VI. Conclusion

In a DC microgrid, several droop controlled paralleled DC/DC converters are installed in distributed substations for transferring power from external grid to the microgrid. Although centralized optimization and decision-making methods can realize power loss reduction and energy efficiency improvement, it may be impractical or costly for dispersed system to have a centralized control system. In order to actualize distributed optimization purposes, this paper proposes a dynamic consensus algorithm based distributed optimization method so as to enhance the overall efficiency of a droop regulated DC microgrid.

Consensus algorithm is used in each local agent for obtaining the global information of total load current and number of online converters. Based on this information, genetic algorithm is applied for decision-making procedure which gives the optimal VR to local controller. Adaptive VR method is applied in primary level so as to follow the VR reference from tertiary level.

HiL results are presented which demonstrate that the proposed method achieves distributed optimization for system overall efficiency enhancement. Consensus algorithm is able to provide accurate and reliable information to each local agent. The priority shifting method realizes the equal workload distribution among converters.

References

[1] A. Bidram and A. Davoudi, "Hierarchical Structure of Microgrids Control System," *IEEE Trans. Smart Grid*, vol. 3, no. 4, pp. 1963–1976, Dec. 2012.

[2] J. M. Guerrero, J. C. Vasquez, J. Matas, L. G. de Vicuna, and M. Castilla, "Hierarchical Control of Droop-Controlled AC and DC Microgrids—A General Approach Toward Standardization," *IEEE Trans. Ind. Electron.*, vol. 58, no. 1, pp. 158–172, Jan. 2011.

[3] T. L. Vandoorn, B. Meersman, J. D. M. De Kooning, and L. Vandevelde, "Analogy Between Conventional Grid Control and Islanded Microgrid Control Based on a Global DC-Link Voltage Droop," *IEEE Trans. Power Deliv.*, vol. 27, no. 3, pp. 1405–1414, Jul. 2012.

[4] L. Meng, T. Dragicevic, J. M. Guerrero, and J. C. Vasquez, "Optimization with system damping restoration for droop controlled DC-DC converters," in *2013 IEEE Energy Conversion Congress and Exposition*, 2013, pp. 65–72.

[5] T. Dragicevic, J. M. Guerrero, J. C. Vasquez, and D. Skrlec, "Supervisory Control of an Adaptive-Droop Regulated DC Microgrid With Battery Management Capability," *IEEE Trans. Power Electron.*, vol. 29, no. 2, pp. 695–706, Feb. 2014.

[6] P. Klimczak and S. Munk-Nielsen, "Comparative study on paralleled vs. scaled dc-dc converters in high voltage gain applications," in *2008 13th International Power Electronics and Motion Control Conference*, 2008, pp. 108–113.

[7] T. Dragicevic, J. Guerrero, and J. C. Vasquez, "A Distributed Control Strategy for Coordination of an Autonomous LVDC Microgrid Based on Power-Line Signalling," *IEEE Trans. Ind. Electron.*, vol. PP, no. 99, pp. 1–1, 2013.

[8] F. Katiraei, R. Iravani, N. Hatziargyriou, and A. Dimeas, "Microgrid Management," *IEEE Power Energy Mag.*, pp. 54–65, 2008.

[9] W. Su and J. Wang, "Energy Management Systems in Microgrid Operations," *The Electricity Journal*. 2012.

[10] S. Russell and P. Norvig, *Artificial Intelligence: A Modern Approach*, vol. 60. 2003, pp. 269–72.

[11] R. Olfati-Saber, J. A. Fax, and R. M. Murray, "Consensus and Cooperation in Networked Multi-Agent Systems," *Proc. IEEE*, vol. 95, 2007.

[12] Y. Xu and W. Liu, "Novel Multiagent Based Load Restoration Algorithm for Microgrids," *IEEE Trans. Smart Grid*, vol. 2, pp. 140–149, 2011.

[13] W. Zhang, Y. Xu, W. Liu, F. Ferrese, and L. Liu, "Fully Distributed Coordination of Multiple DFIGs in a Microgrid for Load Sharing," *IEEE Trans. Smart Grid*, vol. 4, no. 2, pp. 806–815, Jun. 2013.

[14] H. Liang, B. Choi, W. Zhuang, X. Shen, A. A. Awad, and A. Abdr, "Multiagent coordination in microgrids via wireless networks," *IEEE Wireless Communications*, vol. 19. pp. 14–22, 2012.

[15] Q. Shafiee, J. M. Guerrero, and J. C. Vasquez, "Distributed Secondary Control for Islanded Microgrids—A Novel Approach," *IEEE Trans. Power Electron.*, vol. 29, no. 2, pp. 1018–1031, Feb. 2014.

[16] X. Lu, J. M. Guerrero, and K. Sun, "Distributed secondary control for dc microgrid applications with enhanced current sharing accuracy," in *2013 IEEE International Symposium on Industrial Electronics*, 2013, pp. 1–6.

[17] S. D. J. McArthur, E. M. Davidson, V. M. Catterson, A. L. Dimeas, N. D. Hatziargyriou, F. Ponci, and T. Funabashi, "Multi-Agent Systems for Power Engineering Applications—Part I: Concepts, Approaches, and Technical Challenges," *IEEE Trans. Power Syst.*, vol. 22, no. 4, pp. 1743–1752, Nov. 2007.

[18] S. D. J. McArthur, E. M. Davidson, V. M. Catterson, A. L. Dimeas, N. D. Hatziargyriou, F. Ponci, and T. Funabashi, "Multi-Agent Systems for Power Engineering Applications—Part II: Technologies, Standards, and Tools for Building Multi-agent Systems," *IEEE Trans. Power Syst.*, vol. 22, no. 4, pp. 1753–1759, Nov. 2007.

[19] L. X. L. Xiao and S. Boyd, "Fast linear iterations for distributed averaging," *42nd IEEE Int. Conf. Decis. Control (IEEE Cat. No.03CH37475)*, vol. 5, 2003.

[20] S. Sučić, J. G. Havelka, and T. Dragičević, "A device-level service-oriented middleware platform for self-manageable DC microgrid applications utilizing semantic-enabled distributed energy resources," *Int. J. Electr. Power Energy Syst.*, vol. 54, pp. 576–588, 2014.

[21] M. Kriegleder, "A Correction to Algorithm A2 in 'Asynchronous Distributed Averaging on Communication Networks'," vol. PP, no. 99. p. 1, 2013.